TENTH EUROPEAN ROTORCRAFT FORUM

1984 Lichten Award Paper
Selected by the
American Helicopter Society

DEVELOPMENT AND EVALUATION OF A GENERIC ACTIVE HELICOPTER VIBRATION CONTROLLER

Mark W. Davis

Associate Research Engineer
Aeromechanics Research Section
United Technologies Research Center
East Hartford, Connecticut

August 28-31, 1984
The Hague, The Netherlands

The Netherlands Association of Aeronautical Engineers
and
The Department of Aerospace Engineering of
Delft University of Technology

DEVELOPMENT AND EVALUATION OF A GENERIC ACTIVE HELICOPTER VIBRATION CONTROLLER

Mark W. Davis
Associate Research Engineer,
Aeromechanics Research Section
United Technologies Research Center
East Hartford, Connecticut

Abstract

A computerized generic active controller has been developed for alleviating helicopter vibration by closed-loop implementation of higher harmonic control (HHC). This controller provides the capability to readily define many different algorithms by selecting from three control approaches (deterministic, cautious, and dual), two linear system models (local and global), and several methods of limiting control. A non-linear aeroelastic analysis was used to evaluate alternative configurations as applied to a forward-flight simulation of the four-bladed H-34 rotor operating on the NASA Ames Rotor Test Apparatus (RTA), which represents the fuselage. Excellent controller performance is demonstrated for all three control approaches for steady flight conditions, having moderate to high values of forward velocity and rotor thrust. Reductions in RTA vibration from 75 to 95 percent are predicted with HHC pitch amplitudes of less than one degree. Good transient performance and vibration alleviation is also demonstrated for short duration maneuvers involving a sudden change in collective pitch. The existence of multiple HHC solutions to achieve low vibration indicates the potential for calculating solutions that also reduce the detrimental effects of HHC on blade stresses and rotor performance. The effect of controller tuning on system performance is also discussed.

Notation

C_T	thrust coefficient
J	quadratic performance index
J_Z	quadratic vibration performance index
M	mobility matrix between hub and fuselage
P	covariance of identified parameters
P_{TT}	covariance of transfer matrix
P_{TZ}	cross-covariance of transfer matrix and uncontrolled vibration
P_{ZZ}	covariance of uncontrolled vibration
R	covariance of measurement noise; total blade radius
r	blade spanwise location
T	transfer matrix between control inputs and vibration response
V	airspeed
W_Z	vibration weighting matrix
$W_{\Delta\theta}$	rate of change of control weighting matrix
W_θ	control amplitude weighting matrix
Z	vibration response vector in the RTA
Z_H	vibration response vector at the hub (fixed system)
Z_o	uncontrolled vibration response vector
β	indicates control approach in generic algorithms
γ	control vector dependent upon system model (see Eq. (3))
$\Delta\theta$	incremental change in pitch control
$\Delta\theta_{max}$	max allowable change in pitch control
θ	pitch control vector
λ	stochastic control constant
σ	rotor solidity

Subscripts

i	time step or rotor rev
jj	diagonal element of matrix

Superscripts

T	matrix or vector transpose
*	calculated optimum control

Presented at the 40th Annual Forum of the American Helicopter Society, Crystal City, Virginia, May 16-18, 1984.

Investigations leading to the results presented herein were funded by the NASA, Ames Research Center, under Contract NAS2-11260.

Introduction

Commercial utilization of the helicopter is directly affected by both cruise velocity and passenger perception of a "jet-smooth" ride. Thus, increasingly stringent vibration requirements coupled with the desire for high speed aircraft have made vibration alleviation one of the prime objectives of the helicopter industry. The need for further improvements in vibration is readily apparent in the amount of research being conducted and in the diverseness of the approaches being pursued. References 1 and 2 represent the renewed interest in understanding the fundamental sources of vibration and redesigning the blade in order to desensitize it to vibratory rotor airloads. Reference 3 formulates a method for optimizing more conventional procedures that use passive devices, such as vibration absorbers, to desensitize critical points in the fuselage to forces transmitted from the rotor. The potential limitation of these methods is that they may not sufficiently reduce vibration over a wide range of flight conditions.

In contrast to the many passive design procedures currently being pursued, the use of a self-adaptive controller to implement higher harmonic control (HHC) in closed-loop fashion potentially allows significant vibration reduction to be achieved throughout the flight envelope. In this approach, higher harmonic blade root pitch, which can be input through the standard swashplate configuration, is used to modify blade airloads and reduce harmonic blade forcing of the fuselage. Reference 4 presents an excellent review of past helicopter higher harmonic control work. The effectiveness of HHC in reducing vibration was experimentally verified by open-loop wind tunnel model testing in Refs. 5 through 7. In Ref. 8, the loop was closed and vibration was reduced by actively adjusting HHC amplitudes to minimize vibration based on off-line identification of the relationship between vibration and control inputs. References 9 through 11 successfully combined closed-loop HHC with optimal control theory to actively reduce vibration in real-time. References 9 and 10 present the results for a numerical simulation using a nonlinear aeroelastic helicopter vibration analysis, while Ref. 11 presents the results for experimental testing of a model articulated rotor in a wind tunnel.

References 12 through 16 have investigated various aspects of the closed-loop HHC vibration control problem such as the effects of system nonlinearities, errors in initial estimates of system properties, measurement noise, and variations in flight speed on controller stability and performance. These references also proposed a few refinements to the control algorithms used. Finally, Ref. 17 presents the results of a flight test with closed-loop HHC.

While previous research has verified the feasibility, both theoretically and experimentally, of reducing vibration with closed-loop HHC, published work concerned with the refinement and direct comparison of various algorithms is lacking. Such an effort is needed as a step in developing an "optimum" multivariable algorithm for the helicopter vibration problem. The purpose of the investigation reported in this paper is to refine, evaluate, and compare alternative controller configurations in order to more fully understand the effects of tuning parameters within the algorithms and their relative performance. The algorithms selected for evaluation are those shown in previous studies to have the potential for providing effective vibration alleviation. Three control approaches (deterministic, cautious, and dual), two system models (local and global), and various methods of limiting control have been used as the basis of these algorithms. The results presented herein summarize the key findings of the research reported in Ref. 18.

Analytical Simulation of Vibration Controller

Conventionally, higher harmonic control (HHC) is implemented in the main rotor system to modify blade airloads and minimize harmonic vibratory blade forcing of the fuselage. As shown in Fig. 1, higher harmonic blade pitch is input through the standard helicopter swashplate. In the closed-loop system shown, a set of fixed-system sensors measures the resulting vibration response to be provided to an active controller. Based on this response and on-line identification of system parameters, the active controller calculates and commands the HHC inputs required to further reduce vibration in the fuselage. For a four-bladed helicopter rotor, 4/rev vibration in the rotorcraft is minimized by prescribing 4/rev collective and cyclic motions in the non-rotating swashplate, which result in blade cyclic pitch motions at 3, 4, and 5/rev in the rotating system (Ref. 19).

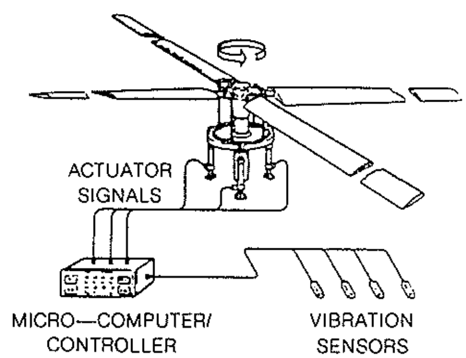

Fig. 1 Active vibration control system.

In the current study, a digital computer simulation of the above vibration control system is used to evaluate and compare the performance of several different controller algorithms. As shown in Fig. 2, this simulation is achieved by linking an existing nonlinear aeroelastic analysis, which simulates the rotorcraft, to a computer subroutine that performs all the functions of the active vibration controller. The rotorcraft simulation and each of the components of the active controller will be discussed separately.

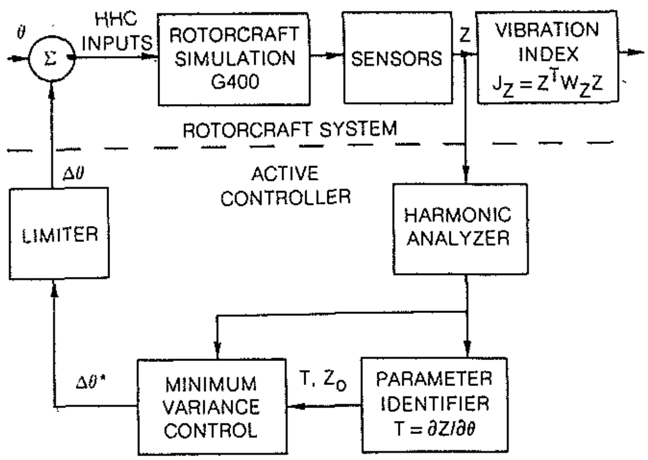

Fig. 2 Simulation of active vibration control system.

Rotorcraft Simulation

The nonlinear aeroelastic analysis used to simulate the rotorcraft is the G400 analysis, documented in Ref. 20. This computer analysis performs a time history solution of the differential equations of motion for a helicopter rotor coupled with a flexible body such as a fuselage. The nonlinear equations of motion are solved by using a Galerkin procedure in which the uncoupled normal modes of the rotor and fuselage are used as degrees of freedom. A feature of G400 which makes it especially suitable for this study of self-adaptive HHC is the capability of computing a transient time history which considers the influence of a flexible fuselage and the motion of each individual blade. For computational efficiency, a constant inflow model has been used in the current study.

Sensors

The simulation of sensor components, used to provide vibration response information to the active controller, is based on calculating linear accelerations at the fuselage hub from the G400 time history formulation. Fuselage accelerations are then calculated from accelerations at the hub (fixed system) by the following linear transformation:

$$Z = M * Z_H \tag{1}$$

For the four-bladed rotor used in this study, Z is a vector of the cosine and sine components of 4/rev acceleration in the fuselage, and Z_H is a vector of the cosine and sine components of 4/rev acceleration at the hub. The mobility matrix M is determined from a steady state forced vibration analysis based on a NASTRAN model of the selected rotorcraft. The computed accelerations are processed by a harmonic analyzer to obtain phase and amplitude relationships. Measurement noise was not simulated in this study.

Active Controller

Six primary controller algorithms are evaluated in this study. These result from three different adaptive control approaches (deterministic, cautious, or dual) for calculating minimum vibration control solutions and from two system models (local or global) which can be used as the basis for each control approach. Regardless of the controller configuration implemented, there are two fundamental characteristics of the active controller: (1) a quasi-static linear transfer matrix (T-matrix) relationship between the vibration response and the HHC inputs is assumed; (2) the T-matrix is identified on-line to account for changes due to system nonlinearities or variations in flight condition. The generic controller used in this study is formulated such that each of the primary algorithms can be implemented according to the value of only two parameters, which indicate the system model and the control approach selected.

It is assumed that a quasi-static linear T-matrix relationship can be defined (for the ith rev) between the higher harmonic pitch and the vibration response. The form of this matrix relationship depends on the system model used to represent the rotorcraft. For the local model the T-matrix is defined by

$$Z_i = T(\theta_i - \theta_{i-1}) + Z_{i-1} \tag{2}$$

In this expression, T is the matrix relating 4/rev fuselage vibration response Z to HHC inputs θ, the harmonics of multicyclic control in the rotating system. This system model is termed the local model to indicate linearization of the T-matrix about the current control point. In contrast, the global model linearizes the system T-matrix about the uncontrolled vibration level Z_o (zero HHC), and the matrix relationship is defined by

$$Z_i = T\,\theta_i + Z_o \tag{3}$$

The algorithm for a given control approach and system model is based on three interrelated operations that perform the controller functions shown in Fig. 2 (e.g., minimum variance control, Kalman filter system identification, and limiting of control inputs). These operations are described in the following sections.

Minimum Variance Control - The required change in the HHC inputs for minimum vibration in the ith sample period is calculated by a minimum variance control algorithm, which is discussed in detail in Ref. 18. This algorithm is based on minimization of a quadratic performance index that consists of a weighted sum of the mean squares of the input and output variables:

$$J = Z_i^T W_Z Z_i + \gamma_i^T (\beta \cdot \lambda \cdot P_i \sum_j W_{Zjj}) \gamma_i + \theta_i^T W_\theta \theta_i + \Delta\theta_i^T W_{\Delta\theta} \Delta\theta_i \quad (4)$$

where $\gamma_i = \Delta\theta_i$ for the local model and $\gamma_i = (\theta_i^T \; 1)$ for the global model. As will be discussed below, β acts as a switching function dependent on the control approach used.

The performance index J is a function of not only the computed harmonics of vibration (Z), but also the pitch control inputs (θ) and the incremental change in control ($\Delta\theta$). In the first term W_Z is a diagonal weighting matrix used to reflect the relative contribution of each vibration component to system vibration levels. It is this term that is indicative of overall effectiveness in reducing vibration. The second term in Eq. (4) is used to modify the controller algorithms to account for uncertainties in identified system parameters according to the underlying assumptions of the control approach being used. These uncertainties are reflected in P_i the covariance matrix calculated by the Kalman filter identification algorithm, which is discussed in the next section. The effect of this stochastic control term is determined by β, and the arbitrary stochastic control constant λ. Finally, in the last two terms, diagonal weighting matrices W_θ and $W_{\Delta\theta}$ are used to inhibit excessive control amplitudes and rates of change in control, respectively. This "internal limiting" is used not only to satisfy hardware requirements, but also to enhance controller performance.

For the deterministic control approach, β is set to zero, since all system parameters are assumed to be explicitly known. This approach ignores the fact that only estimates for the T-matrix (and Z_o for the global model) are available from the parameter identifier. The performance of the deterministic controller is tuned by appropriate selection of the elements of the weighting matrices (W_Z, W_θ, $W_{\Delta\theta}$) discussed above.

In the cautious approach, which was suggested and experimentally evaluated in Refs. 11 and 12, it is recognized that some of the system parameters are only estimates, and control inputs are implemented more cautiously than for the deterministic approach. This is accomplished by setting β equal to one. The result for the local model is a positive stochastic control term having a similar effect to that of the $W_{\Delta\theta}$ term. The rate-limiting effect due to this term will depend on the uncertainty in the identified T-matrix, as reflected by P_i. As system identification becomes worse, this controller becomes more cautious. As system identification improves and P_i goes to zero, the performance index reduces to that for the deterministic controller. For the global model, the stochastic control term places a constraint on control magnitude similar to that of W_θ. Again, the limiting of θ due to this term will depend on the uncertainty in system identification. Note that a stochastic control constant λ has been added in both cases to allow for empirical modification of the amount of caution provided by the controller.

The last control approach to be evaluated in this study is an active adaptive formulation (Ref. 21), also known as a dual controller (Ref. 22). While the cautious controller accounts for parameter uncertainties, it does not directly affect identification. The dual controller, on the other hand, attempts to improve long term system identification by actively probing the system while at the same time providing good control. Since optimal dual controllers are generally too complex to be practical (Refs. 4 and 23), the dual controller used in this study is a suboptimal approach taken from Ref. 22, with β set to $(-1/R \cdot \sum W_{Zjj})$. The resulting stochastic control term is $-\gamma_i^T (\lambda \cdot P_i / R) \gamma_i$ where γ_i is defined as above, and R is the covariance of the measurement noise used in the Kalman filter identification algorithm. The overall effect of this term is a reduction in the weighting placed on the rate of change of control for the local model and on the control magnitude for the global model. Whereas the cautious controller penalizes control when identification is poor by increasing constraints, the dual controller increases control by a reduction in constraints. The result is system probing used by the dual controller to improve system identification. The relaxed internal constraints on control are dependent on the ratio of the uncertainty in the identified system parameters to the uncertainty in the computed vibration response. As system identification improves and P_i goes to zero, the stochastic dual control term vanishes and system probing ceases. As discussed in Ref. 23, the two tasks of trying to improve system identification and of trying to provide good control are, in general, counter-productive. Good identification may require large control inputs, while good control may require small control inputs. Thus, the arbitrary stochastic control constant λ is used to tune the dual controller in order to achieve an acceptable tradeoff, where short term control may be compromised.

While the form of the performance index depends on the control approach and the system model used, the method for obtaining the minimum variance control algorithm is the same for any particular configuration. Once the performance index has been established by substituting the appropriate expression for Z_i from Eqs. (2) or (3), the minimum variance control algorithm is then obtained by taking the partial derivative of the resulting expression for J with respect to θ_i, and setting it equal to zero. The result can be solved for $\Delta\theta_i^*$ where the superscript * denotes the optimal HHC input required for minimum variance. The closed form controller solution for all three control approaches can be written for the local system model as

$$\Delta\theta_i^* = -D\ [W_\theta\ \theta_{i-1} + T^T W_Z\ Z_{i-1}] \quad (5)$$

and for the global model as

$$\Delta\theta_i^* = -D\ [(T^T W_Z T + W_\theta + \beta\cdot\lambda\cdot P_{TT} \sum_j W_{Zjj})\theta_{i-1} + T^T W_Z\ Z_o + \beta\cdot\lambda\cdot P_{TZ} \sum_j W_{Zjj}] \quad (6)$$

where the expression D in both models can be defined as

$$D = (T^T W_Z T + W_\theta + W_{\Delta\theta} + \beta\cdot\lambda\cdot P_{TT} \sum_j W_{Zjj})^{-1} \quad (7)$$

Note that the update in control for the local model is dependent on an estimate of the T-matrix and the computed vibration response from the last update Z_{i-1}. For the local model, P_{TT} is the covariance of the T-matrix, which is simply covariance, P_i, since only the T-matrix is identified. For the global model, the control update is based on an estimate of both the T-matrix and the uncontrolled vibration response Z_o. In Eq. (7), P_{TT} is again the covariance of the T-matrix, which is now a sub-matrix of P_i since both T and Z_o are identified. P_{TZ} is the cross-covariance of T and Z, which is also a sub-matrix of P.

Kalman Filter System Identification - Accurate identification of the T-matrix, as well as Z_o for the global model, is important for good vibration reduction, since the minimum variance control algorithms all depend explicitly on the estimates of these parameters. The method used for estimating and tracking system parameters is discussed in detail in Ref. 18.

Identification of the T-matrix is obtained by considering each row of matrix Eq. (2) or (3) as the state vector of a separate identification problem. For the global model, the problem is modified slightly by adding each component of Z_o to the corresponding state vector. The state vectors are then treated as time-varying quantities which must be tracked to account for changes in system parameters due to system nonlinearities and changes in flight condition. At the beginning of each sample period, the state vectors are updated by a correction term that is proportional to the difference between the G400 computed and the estimated vibration levels. The proportionality constants or Kalman gains are calculated according to the Kalman filter algorithm and are dependent upon the ratio between the uncertainty in the estimated T-matrix and the uncertainty in the computed vibration response.

Regardless of which system model is used, the Kalman filter identification algorithm requires only the current vibration response and error covariances to identify the required system parameters. Therefore, the procedure can be carried out recursively with information from only the present and the previous sample periods. The importance of this characteristic is that implementation can easily be carried out in real time for transient maneuvers. However, this recursive characteristic of the controller requires that the controller be initialized at the time it is activated. In the present study, the initial T-matrix determined from open-loop perturbation at the baseline flight condition is used for all flight conditions.

Limiting of Control Inputs - There are several reasons for limiting control inputs. In an actual rotorcraft, limiting will be necessary to satisfy hardware requirements of the actuators used to implement HHC. The total amplitude of control must also be constrained to satisfy mechanical stress and safety requirements. Beyond the practical aspects of limiting control inputs, rate-limiting has been found to be very important to enhance controller stability and performance for nonlinear systems or for systems where initial parameter estimates are poor.

Figure 2 shows that the active controller externally limits the optimum control inputs calculated by the minimum variance control algorithm before implementing them in the rotorcraft simulation. This is referred to as external limiting since it is done outside the minimum variance control algorithm and without regard to optimality. With external limiting, satisfaction of absolute control limits can be ensured. This is in contrast to internal limiting which is accomplished by weighting θ and $\Delta\theta$ in the performance index. By appropriate tuning of these weighting matrices, W_θ and $W_{\Delta\theta}$, it is possible to take into account the desire to satisfy constraints on control magnitude and rates of changes while calculating the optimum solution. However, internal limiting can only inhibit control. It can not ensure satisfaction of absolute limits. Thus, in practice, provision for external limiting would also be required. In this study, a comparison is made between these two methods of limiting control and their effect on controller performance.

Controller Implementation

Once the controller is activated, it calculates and updates the required higher harmonic pitch control once every sample period. In this study, a 1 rev update is used. At the start of a typical rotor rev, a step change in HHC input is implemented and the resulting transient response is allowed to decay for 3/4 rev before activating the harmonic analyzer. This delay is necessary to improve the accuracy of information provided to the parameter identifier. While the 3/4 rev allowed for transient decay is somewhat arbitrary, it has proven to be a good tradeoff between the desire for accurate system identification and the desire to update as often as possible. The time history of the vibration response is sampled for the last 1/4 rev and read into the harmonic analyzer, which calculates and supplies the cosine and sine components of each vibration component to the parameter identifier. Based on the vibration response and identified parameters from the last rev, the controller updates system identification, calculates the required higher harmonic control, and commands an updated HHC input which takes the form of a new $\Delta\theta$ step input implemented at the beginning of the next rev. This procedure is repeated recursively throughout the entire flight, including all maneuvers.

Analytical Results

In the present study, the aeroelastic simulation of the rotorcraft is based on a fully articulated, four-bladed H-34 rotor (see Ref. 24 for physical description) mounted on the Rotor Test Apparatus (RTA), which is used to represent the fuselage in full scale rotor tests in the NASA-Ames 40' x 80' wind tunnel. The normal vibration mode data, needed by the G400 aeroelastic analysis to represent the flexible RTA, was obtained from an existing NASTRAN mathematical model provided by NASA. This model includes not only the RTA structure, but also the wind tunnel support struts and balance frame. Descriptions of the six modes used to represent the RTA are provided in Ref. 18. Vibration response information to be provided to the active controller are calculated at six locations throughout the RTA. The location and orientation of each vibration component are shown in a simplified schematic of the RTA in Fig. 3. Since

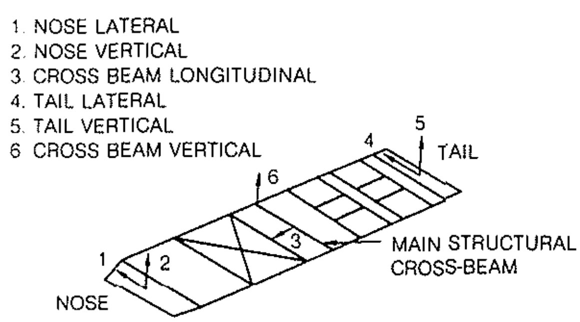

Fig. 3 Location and orientation of vibration components in rotor test apparatus.

these components include three orthogonal directions and are widely spread out in the RTA, their reduction should be indicative of overall vibration reduction in the RTA.

A steady level-flight condition was selected for the initial tuning and evaluation of all six primary controller configurations. This flight condition had a forward velocity of 150 kt and a nominal value of 0.058 for C_T/σ. Based on these results, a representative baseline controller configuration was selected for each of the three control approaches. The characteristics of each of these controllers are presented in Table 1.

Table 1. Baseline controller configurations

	Deterministic	Cautious	Dual
System Model	Global	Global	Global
External Control Limits			
θ_{max} (deg)	none	none	none
$\Delta\theta_{max}$ (deg/rev)	none	none	0.2
Stochastic Control Constant (λ)	0.0	1.0	0.01
Weighting in Perf. Index			
Sensors, W_Z $(1/g's)^2$	1.0	1.0	1.0
Control Magnitude, W_θ $(1/rad)^2$	0.0	0.0	0.0
Change in Control, $W_{\Delta\theta}$ $(1/rad)^2$	1000.	0.0	0.0

All three baseline controllers are based on the global system model, although there is no significant advantage of one model over the other at this flight condition. Other than the control approach and the related stochastic control constant λ, the only difference between these three controllers is the manner in which limiting of control inputs is implemented. The deterministic controller slows the rate of change of control inputs between updates by internally weighting $\Delta\theta$ with equal values of $W_{\Delta\theta}$ for 3, 4 and 5/rev pitch amplitudes. The value of $W_{\Delta\theta}$ in Table 1 allows the deterministic controller to maintain an acceptable rate of change in control on the order of 0.2 deg/rev. The cautious controller uses neither external nor internal $\Delta\theta$ limiting, but inherently slows down the implementation of new control inputs via the stochastic control term discussed previously. The dual controller uses external limits of 0.2 deg/rev on the rate of change of control to allow the inherent perturbations in control inputs to occur without excessively compromising short term control. These baseline controller configurations are evaluated in the following sections.

Baseline Flight Vibration Reduction

Figure 4 presents the G400 simulation results for each of the three baseline controller configurations operating closed-loop at the baseline 150 kt flight condition. The simulation includes three revs of uncontrolled flight to allow initial numerical transients to die out before activating each controller at rev 4. Figure 4 shows G400 predicted time histories of the vibration performance index J_Z and the amplitude of the 3/rev HHC input commanded by each baseline controller. While not shown, 4 and 5/rev inputs commanded by each controller have similar time histories to those shown for 3/rev. Since the vibration performance index is a weighted sum of the squares of all the vibration components being actively controlled; it is a good indicator of overall controller performance in reducing vibration. Note that the vibration performance index (J_Z) plotted is not the same as the performance index (Eq. (4)) actually minimized by the control algorithms, since none of the quadratic terms involving θ or $\Delta\theta$ are included. While these terms are important to overall controller performance and stability, they are not indicative of vibration reduction achieved by the active controller. All the performance index plots in this paper are based on J_Z.

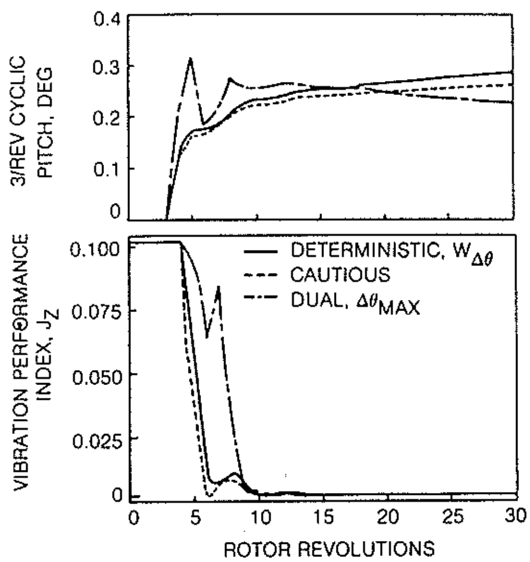

Fig. 4 Time history of vibration index and 3/rev control at baseline flight condition (V=150 kt, C_T/σ=0.058).

Figure 4 shows that all three controllers do an excellent job of reaching a new steady vibration level that is greatly reduced from the uncontrolled vibration level at rev 4. After the controller is activated, the vibration performance index J_Z immediately starts to decrease for all three controllers. After only two revs and 0.55 seconds elapsed time of active control, both the deterministic and cautious controllers achieve and maintain at least a 90 percent reduction in the performance index. The dual controller requires about 5 revs or 1.4 seconds of active control to achieve the same overall vibration level. By rev 10, all three controllers have essentially converged to a value of the performance index that is only 3 percent of the uncontrolled value.

Figure 4 also shows the time history of 3/rev HHC amplitude as commanded by the three controllers. The deterministic and cautious controllers smoothly increase the amplitude of all three control inputs, while continually reducing the vibration level. After rev 15, the vibration at the six RTA sensor locations remains fairly steady. At this point, the 3/rev cyclic pitch amplitude is still rising slowly. While not shown, the 4/rev input is decreasing at a comparable rate and 5/rev remains fairly steady. Thus, after 15 revs, both the deterministic and cautious controllers are trying to further reduce vibration but, in effect, achieve a fairly steady vibration level by trading off an increase in 3/rev with a decrease in 4/rev cyclic pitch. While this slight tendency to drift may be eliminated by implementing and tuning W_θ in the performance index, all the time history solutions presented in this paper were obtained without any W_θ weighting.

In contrast to the deterministic and cautious controllers, the dual controller exhibits a tendency to probe the system by perturbating the higher harmonic cyclic inputs. This tendency is clearly evident in the cyclic pitch amplitude shown in Fig. 4. As expected, this probing initially results in a slight degradation in short term control as can be seen in the performance index. After identification improves, system probing diminishes and the final controller solution is as good as that of the deterministic and cautious controllers. The dual controller's tendency to probe the system has been somewhat inhibited by an application of external rate limits of 0.2 deg/rev, as shown in Table 1. Without these limits, the perturbation in control inputs used to probe the system are much larger and result in much worse short term control. A completely unlimited dual controller commanded initial inputs on the order of 1.0 degree and allowed the vibration performance index to increase to sixty times the uncontrolled value before converging to a final solution.

The change in the vibration level at all six locations in the RTA is shown in Fig. 5 for all three controllers. In this figure, the uncontrolled 4/rev vibration levels at rev 4 are compared to those at rev 30 with active control. All three controllers have substantially reduced vibration at all locations except the two that had very low initial levels of vibration. The low levels of vibration at these two locations have been maintained. Reductions in vibration for the four primary components are between 75 and 95 percent.

Also shown in Fig. 5 are the fixed system hub vibrations. Note that angular vibrations have been multiplied by 1 ft to be plotted in g's in this figure. The two largest contributors (vertical and longitudinal) have been reduced by all three controllers. A substantial 75 percent decrease in the longitudinal component has been achieved, while a more modest 20 percent reduction has been achieved in the vertical component. The other four components, which were smaller initially, remain at about the same levels. This indicates that the reductions in vibration in the RTA have been achieved by a combination of reduced forcing at the rotor hub and vectorial cancellations of hub component contributions to RTA vibrations.

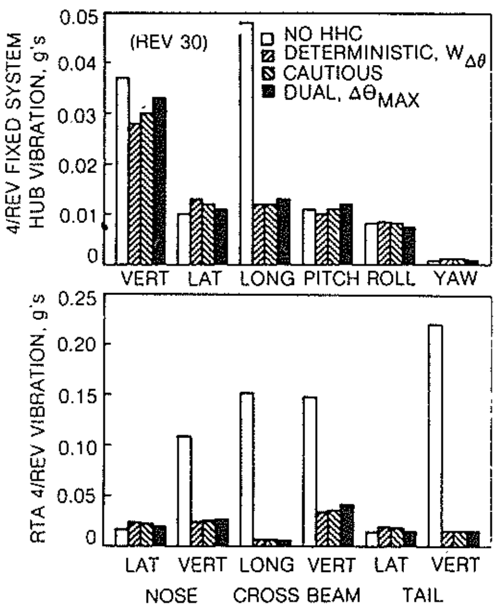

Fig. 5 Effect of active control on 4/rev vibration at baseline flight condition (V=150 kt, C_T/σ=0.058).

Effect of Forward Velocity

The effect of forward velocity on controller performance is shown in Fig. 6, which compares the time histories of the vibration performance index and 3/rev cyclic pitch amplitude for the baseline cautious controller at three different velocities: 112, 130, and 150 kt. All three flight conditions have the same nominal value of 0.058 for C_T/σ. The cautious controller exhibits the same excellent performance characteristics at all three velocities. Convergence to an acceptable control solution occurs quickly and smoothly within about 5 revs at all three flight conditions. These results have been obtained with no retuning of the controller and with the same initial T-matrix developed at the baseline (150 kt) condition. The controller is very effective at reducing overall vibration at all three velocities with at least a 97 percent reduction in the vibration performance index compared to uncontrolled values. The reductions achieved at each of the RTA locations are shown in Fig. 7 for the two lower velocities. These results can be compared to those already shown for the 150 kt condition and the cautious controller in Fig. 5. At least a 75 to 95 percent reduction has been achieved at all sensor locations except those having low initial levels of vibration with zero HHC (nose and tail lateral).

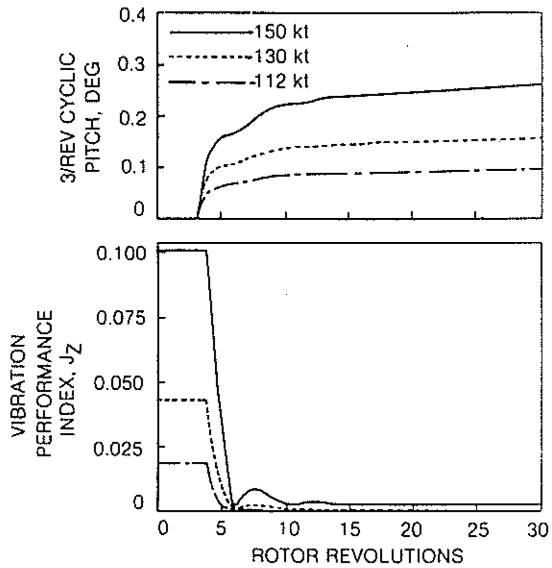

Fig. 6 Effect of forward velocity on cautious controller performance (C_T/σ=0.058).

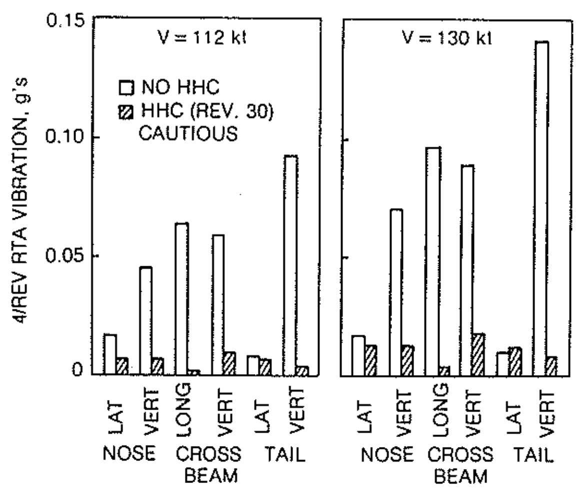

Fig. 7 Effect of forward velocity on 4/rev vibration (C_T/σ=0.058).

The HHC pitch amplitudes required to achieve these substantial reductions increase with forward velocity. The required 3, 4, and 5/rev pitch amplitudes commanded by the baseline active controllers all tend to be of the same order of magnitude when equally weighted in the performance index. The required amplitudes are on the order of

0.1, 0.15, and 0.25 degree at the 112, 130, and 150 kt flight conditions, respectively.

Effect of Rotor Thrust

The effectiveness of the active controller has also been investigated at two more severe flight conditions having the same 150 kt velocity as the baseline (C_T/σ = 0.058) case, but nominal values of 0.08 and 0.085 for C_T/σ. The highest thrust level (C_T/σ = 0.085) is especially severe with a significant increase in vibratory response over both the baseline and intermediate thrust conditions, as shown in Fig. 8. The severity of this condition is due to its being well into stall. As shown in a separate open-loop study in Ref. 18, this flight condition is also more nonlinear, has more aerodynamic interharmonic coupling effects, and has a significantly different T-matrix than the baseline flight condition. Despite this, the baseline controller configurations have been applied without any retuning of the controllers and with the same initial T-matrix developed at the baseline flight condition.

Figure 8 indicates the effectiveness of the baseline controllers in minimizing vibration for all three thrust levels. While the results shown are for the deterministic controller, comparable results were also observed for both the cautious and dual controllers. This figure compares the uncontrolled values of the vibration performance index and 4/rev acceleration at a representative RTA location to the final values at rev 30 with active control. Percentage reductions in the performance index increase with rotor thrust, with at least a 97 percent reduction achieved throughout the range of thrusts considered. Figure 8 also shows at least a 75 percent reduction in vibration at the cross-beam vertical location. More extensive reductions are achieved at all other locations

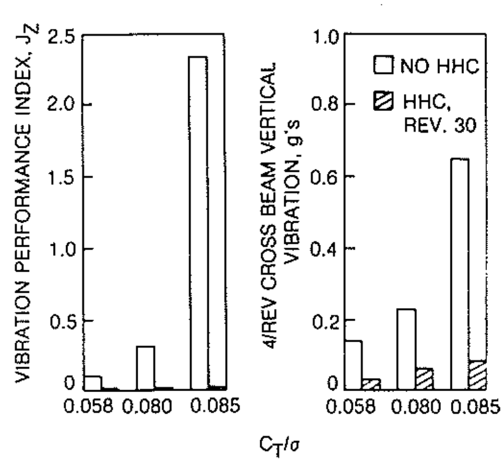

Fig. 8 Effect of rotor thrust on deterministic controller performance (V=150 kt).

except the two lateral accelerations, where low initial vibration levels are maintained. The required amplitudes of 3, 4, and 5/rev control increase with thrust, but are less than 1.0 degree for all thrust levels.

The controllers exhibit virtually the same transient behavior for the intermediate thrust level (C_T/σ = 0.08) as at the baseline flight condition. Due to the inaccurate T-matrix and the stall effects mentioned above, the behavior of all three controllers is somewhat irregular for C_T/σ equal to 0.085. This is exhibited in the time histories of the vibration performance index and the amplitude of the 3/rev pitch shown in Fig. 9. Despite these effects, all three controllers immediately achieve and maintain significant reductions in vibration. As shown in Fig. 9, only 5 revs (1.4 seconds) are required to achieve and maintain at least a 80 percent reduction in the performance index.

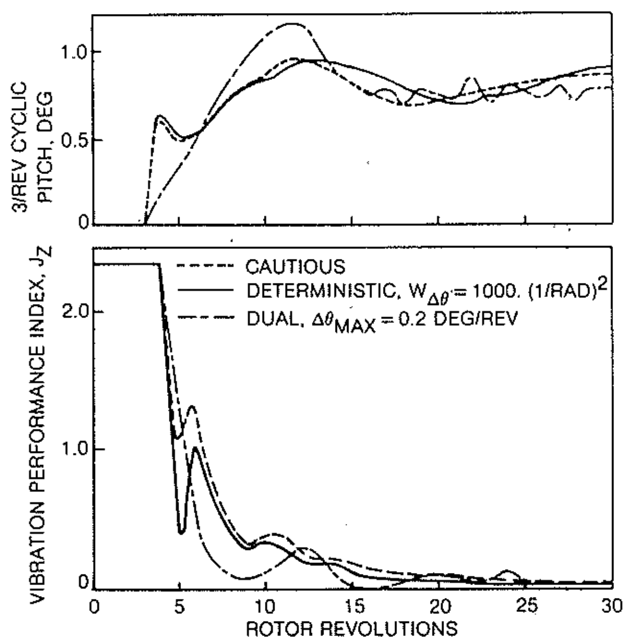

Fig. 9 Time history of vibration index and 3/rev control at high thrust condition (V=150 kt, C_T/σ=0.085).

Controller Performance During High Speed Maneuvers

Each of the three baseline controllers has been evaluated during several short duration maneuvers while using the same initial T-matrix and tuning developed at the steady baseline condition. Each of the maneuvers represents an increase in rotor thrust from the initial steady baseline condition, C_T/σ = 0.058, via step and ramp changes in collective pitch during an otherwise steady flight condition at 150 kt. After all the transients from the sudden change in collective pitch subside, the resulting steady flight condition is one of the high thrust conditions just discussed (C_T/σ = 0.08 or 0.085). For each of these maneuvers, the active vibration controllers not only remain stable, but converge to an excellent control solution having about the same substantially reduced RTA vibration levels as those presented previously for the steady flight conditions.

2.18 Degree Step Increase in Collective Pitch - Figure 10 shows the time histories of 3/rev cyclic pitch and the vibration performance index of all three baseline controllers in response to a 2.18 degree step increase in collective pitch. The simulated maneuver is identical to that shown in Fig. 4 for the first 18 revs. The 2.18 degree step increase in collective pitch occurs at rev 19. The resulting flight condition, after all transients die out, is the same as the highest thrust flight condition ($C_T/\sigma \approx$ 0.085) presented in the last section. At the beginning of rev 20, the controller makes its first update in response to the transient maneuver. After rev 20, the controller actively reduces vibration just as it did for the steady flight conditions, and no further maneuvers are encountered.

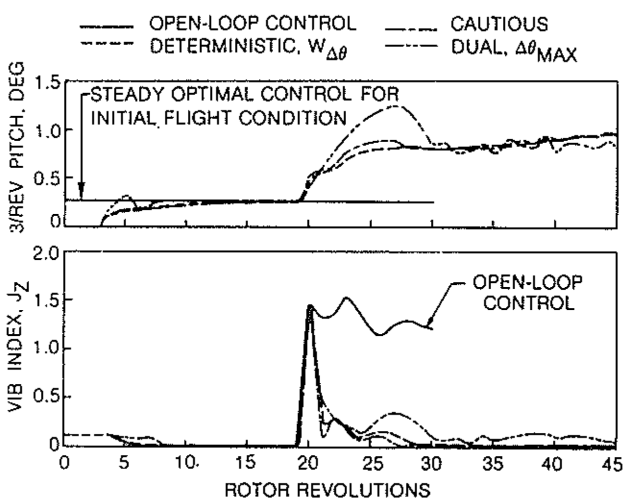

Fig. 10 Controller performance during transient maneuver for 2.18 degree collective step increase (V=150 kt).

The solid line shown in Fig. 10 represents a simulation of open-loop control for the maneuver just described. The HHC inputs implemented for the baseline flight condition remain fixed during and after the maneuver. Thus, any changes occurring in the performance index after rev 19 for the open-loop simulation are due to increased vibration response and transient effects caused by the change in collective pitch.

Despite the large increases in vibration that occur at rev 19 for the 2.18 degree step increase in collective pitch, all three baseline controllers not only remain stable, but immediately start reducing vibration as soon as the 1 rev of dead time used for transient decay, signal sampling, and harmonic analysis is over. The deterministic and cautious controllers achieve and maintain at least an 80 percent reduction in the vibration index relative to peak values in just 2 revs. Again, the behavior of the deterministic and cautious controllers is very similar. The dual controller cannot maintain this level of reduction until rev 29, due to system probing.

All three controllers minimize the transient effects of this maneuver to the point allowed by the 1 rev update, and the peak value of the performance index has been kept well below the uncontrolled value of 2.33 for the final flight condition. It may be possible to reduce the peak response further by shortening the time between updates, since the controllers could then start to reduce vibration sooner. However, the tradeoff is the increased transient effects on the harmonically analyzed vibration signals.

2.18 Degree Ramp Increase in Collective Pitch - Figure 11 shows the response of two cautious controllers to a transient maneuver that has the same initial and final flight conditions as the 2.18 degree step change in collective pitch just discussed. However, this maneuver involves a ramp increase at a rate of 0.44 deg/rev for 5 revs, beginning at rev 19. The cautious controllers shown are the same except for the tuning of λ. The controller with a value of 1.0 for λ is the baseline.

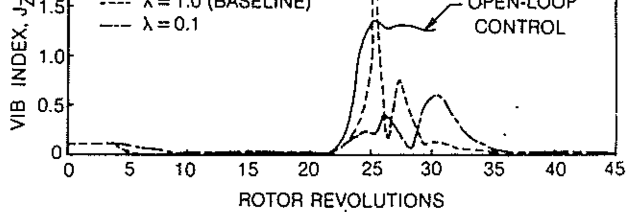

Fig. 11 Cautious controller performance during transient maneuver for 2.18 degree collective ramp increase (V=150 kt).

Both cautious controllers perform satisfactorily in reducing vibration for the first four revs of the maneuver. During this time, the controllers maintain significantly lower levels of vibration than the open-loop values. However, when the last 0.44 degree change in collective pitch is implemented between revs 23 and 24, the result is a significant increase in the calculated baseline controller (λ=1.0) performance index at rev 24, as indicated in Fig. 11. From there on, performance of the baseline controller is not good for about 5 revs. Although it converges to an excellent control solution, a peak value of the performance index is incurred that is larger than those for the open-loop controller and those experienced for the 2.18 degree step increase in collective pitch. While the baseline transient performance shown in Fig. 11 is undesirable, it should be noted that peak vibration levels are below those that would occur if no HHC were implemented.

While it is possible that a different Kalman filter tuning will be required to better track the type of changes in system parameters that are encountered in the stall regime, that approach was not explored in this investigation. Retuning of the minimum variance control algorithm for improved controller performance has been explored briefly. Figure 11 demonstrates that controller performance can be improved significantly during this maneuver by only slightly retuning the minimum variance control algorithm. A smaller value of λ allows the controller to make somewhat larger changes in control early in the maneuver when system identification is still good. In so doing, slightly larger reductions in vibration are achieved in the first 4 revs of the ramp increase in collective pitch. Furthermore, the larger changes in control give the potential to better identify changes in system parameters in the early part of the maneuver. While this controller (λ=0.1) experiences some undesirable transient effects, it converges quickly, while substantially reducing peak and final levels of vibration. The same type of reduction in limiting on control inputs also provides substantially improved performance in the deterministic and dual controllers, again at the expense of large control inputs.

The baseline controllers were also subjected to similar but smaller step and ramp changes in collective pitch resulting in the intermediate thrust condition (C_T/σ = 0.08) discussed above. Transient vibrations were reduced significantly without any retuning of the baseline controllers. For example, this 40 percent increase in thrust was input with a ramp increase in collective pitch at a rate of 0.2 deg/rev for 5 revs. For this maneuver, the controllers reduced peak values of the performance index by over 80 percent of the open-loop values. These maneuvers may be a fairer test of the baseline controllers due to such severe stall effects predicted at the highest thrust condition.

Rotor Blade Stresses

Figure 12 shows the 1/2 peak-to-peak blade bending stresses and torsional moment along the blade span for the baseline flight condition with no HHC and for the deterministic controller at rev 30 with optimum HHC. There is a significant increase in all the vibratory moments and stresses, but especially in the torsional moment, which has more than doubled near the blade root. The inboard flatwise and edgewise bending stresses increase by about 15 and 50 percent, respectively. The effect of the cautious and dual controllers is almost identical to that shown for the deterministic controller.

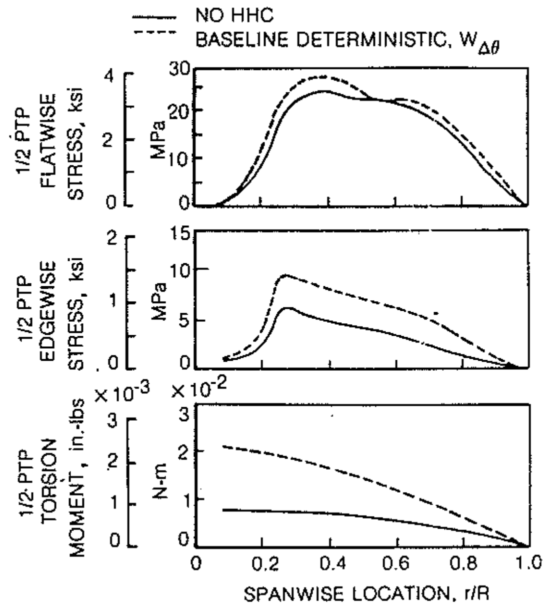

Fig. 12 Effect of active vibration control on rotor blade vibratory moments and stresses at baseline flight condition (V=150 kt, C_T/σ=0.058).

The effect of higher harmonic control on rotor blade stresses varies with flight condition. The relative increase in blade stress and moments caused by HHC increases with flight speed for the 112 to 150 kt range considered. This is most likely due to the larger amplitudes of control required for vibration reduction as velocity increases. For the high thrust conditions (C_T/σ = 0.08 and 0.085), the effect of HHC on blade stresses and moments is inconclusive. The effect of HHC on rotor blade stresses at the highest thrust condition (C_T/σ = 0.085) is shown in Fig. 13 for two different control solutions. The first solution shown was obtained by the same baseline deterministic controller used for the high thrust results shown in Figs. 8 and 9. The second solution was achieved by arbitrarily eliminating 5/rev control with large internal weighting. The relative increases in

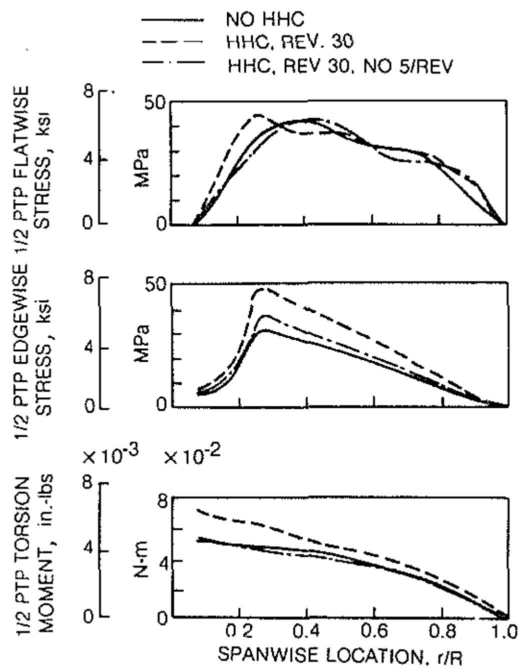

Fig. 13 Effect of active vibration control on rotor blade vibratory moments and stresses at high thrust flight condition (V=150 kt, C_T/σ=0.085).

stress for both control solutions are not nearly as great at this flight condition as they were for the baseline condition. This is especially true for the solution having no 5/rev control, which resulted in almost no increase in the flatwise bending stress and the torsion moment and only about a 20 percent increase in edgewise bending stress. These results suggest that the penalty of increased dynamic blade loads associated with HHC may be reduced by tailoring of HHC inputs. It may also be possible to alleviate these increases in stress, without compromising vibration reduction, by including appropriately weighted terms representative of blade stresses in the performance index J. While such an approach was not pursued in the present study, certain results did indicate that this approach might be feasible. For example, multiple control solutions resulting in similar vibration reductions, but having different effects on rotor blade stresses, have been obtained. One such solution is the solution just discussed, where 5/rev inputs were eliminated.

Rotor Performance

At the baseline flight condition, the application of HHC causes an increase in required torque on the order of about 5 percent for all controllers. For this particular flight condition, a direct power penalty is being paid for the implementation of HHC to reduce vibration (exclusive of any increase in power necessary to operate the control system). It may be possible to guide the controller to a better control solution in terms of rotor performance by including an appropriately weighted term that is indicative of rotor torque in the performance index.

Local vs Global System Model

All the results presented above are for the global system model. The results and accompanying discussion for steady flight conditions are generally applicable to the local system model as well. It is not until controller performance is evaluated during the short duration maneuvers considered in this study that any significant difference in controller behavior due to system model is noticed. For example, without retuning of the controllers, the local model is much more oscillatory and takes longer to converge than the global model for the 2.18 step change in collective pitch. While it is anticipated that these local controllers can be retuned to achieve basically the same performance as the global baseline controllers, this may indicate that the local model is more sensitive to tuning at different flight conditions or perhaps more sensitive to inaccurate vibration response information due to large transient effects.

Effect of Controller Tuning

The tuning of internal controller parameters can have a significant impact on all the important characteristics of controller performance. In this study, the effects of $W_{\Delta\theta}$ and W_θ on the deterministic controller and of λ for the cautious and dual controllers were studied in some detail. Since only a brief summary can be presented here, Ref. 18 should be consulted for more details.

Internal Rate-Limiting - The use of internal rate limiting dramatically improves the stability and performance of the deterministic controller. This is quite apparent in Fig. 14, which compares the overall performance of the baseline deterministic controller (with internal rate-limiting) to that of an externally rate-limited deterministic controller at the baseline flight condition. The externally limited controller has the same configuration as the baseline controller, except that $W_{\Delta\theta}$ is set to zero, $\Delta\theta_{max}$ is set to 0.2 deg/rev, and the local system model is used. The results shown here are the best that could be obtained for an externally limited controller at this flight condition. The baseline controller significantly improves controller performance according to all criteria: much greater vibration reduction in the first step of active control; faster convergence; significantly greater reduction in vibration at convergence; and smaller final control inputs. While external limiting results in comparatively worse controller performance, it should be noted that it reduces the performance index by about 85 percent. The primary reason for the dramatically improved performance achieved by the internally rate-limited controller is that the minimum variance control algorithm takes directly into account the desire to implement relatively small changes in control, when calculating a new solution. In contrast, the arbitrary external limiting of control, without regard to optimality, can cause a very different "mix" (both amplitude and phase) of 3, 4, and 5/rev control to be commanded than that calculated for minimum variance.

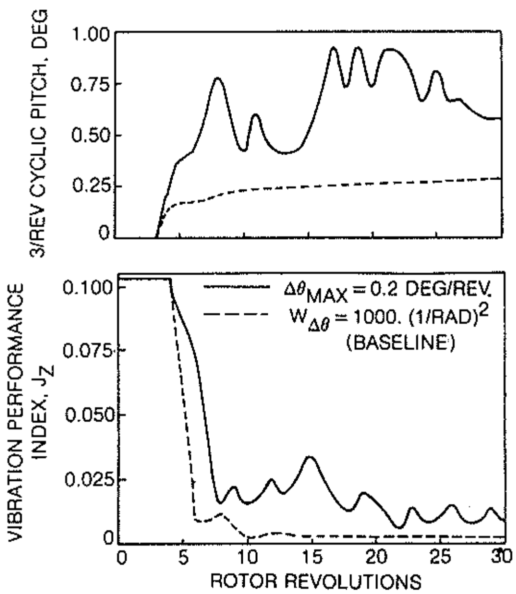

Fig. 14 Comparison of deterministic controller performance with external and internal rate-limiting at baseline flight condition ($V=150$ kt, $C_T/\sigma=0.058$).

The results shown for the baseline controller are for optimal tuning of $W_{\Delta\theta}$. Other tuning values can have a significant impact on controller performance. For small values of $W_{\Delta\theta}$ and without other limiting, the deterministic controller performance is quite oscillatory. However, even minimal internal rate-limiting allows the controller to converge at the baseline flight condition, although the result is a control solution with very large control amplitudes (3.5 degrees). In Ref. 18, it is shown that large control inputs such as these have a much more severe impact on vibratory blade stresses and rotor performance than equally effective small amplitude solutions, even though virtually the same levels of vibration are achieved in the RTA. At the other extreme, very high values of $W_{\Delta\theta}$ cause very slow, smooth reductions in vibration, which may prove too slow for maneuvers. Between these two extremes, moderate values for $W_{\Delta\theta}$, such as those used for Fig. 14, result in very effective control at the many different flight conditions considered in this study. While $W_{\Delta\theta}$ has a significant impact on rate of convergence, it does not impact overall effectiveness in reducing vibration, since it does not inhibit the magnitude of control inputs that can be commanded. The effects of $W_{\Delta\theta}$ on cautious and dual controllers are comparable to those for the deterministic controller. However, it should be noted that internal rate-limiting tends to eliminate the inherent system probing used by the dual controller to enhance system identification. For the cautious controller, internal rate-limiting due to $W_{\Delta\theta}$ complements the built-in caution.

<u>Internal Limiting of Control Magnitude</u> - Internal limiting of the magnitude of control inputs can also dramatically affect the performance of the deterministic controller. This limiting is achieved by weighting θ in the performance index with W_θ to reduce control amplitudes as much as possible without paying an excess penalty in the form of larger vibrations. For small to moderate values of W_θ, the controller is still able to achieve about the same overall vibration reduction with smaller, but properly phased control inputs. However, the value of W_θ can be made too large, such that the controller cannot command sufficient amplitudes to reduce vibration effectively. The value of W_θ has very little effect on rate of convergence, if large enough to prevent undue oscillatory behavior. The deterministic controller tends to be slightly sensitive to the tuning of W_θ.

The effects of W_θ weighting can be used to tailor HHC inputs by unequal weighting of 3, 4, and 5/rev control inputs. This was explored in Ref. 18 by using internal weighting to inhibit or eliminate various control inputs. In Ref. 18, it is shown that many significantly different control solutions can result in very effective vibration reduction in the RTA for the same flight condition. For example in Fig. 13, the effect of two very different HHC solutions on vibratory blade stresses is shown at the high thrust condition. Each of these solutions achieves about the same vibration reduction in the RTA, but affects blade stresses to a different degree. These results indicate that it may be possible to guide the controller to more satisfactory solutions in terms of other criteria (e.g., blade stresses or rotor performance), without severely compromising vibration reduction, by placing appropriate terms in the performance index or using unequal W_θ weighting.

<u>Effect of Stochastic Control Constant</u> - The stochastic control constant λ has a significant effect on the cautious controller performance in much the same way that $W_{\Delta\theta}$ and W_θ effect the deterministic controller, since the stochastic caution term increases the effective weighting on $\Delta\theta$ or θ. For small values of λ, controller performance is oscillatory, but stability is maintained, and

effective control solutions are reached with substantial reductions in vibration. Large values of λ cause very slow, smooth reductions in vibration, which may be too slow for maneuvers. Between these two extremes, a wide range of values for λ results in very effective controllers at the baseline 150 kt flight condition. The stochastic control constant λ also has a large effect on the dual controller. This constant must be tuned to reach an acceptable compromise between good short term control and system probing. At the baseline flight condition, the dual controller is extremely sensitive to the value of λ.

Conclusions

A computerized generic active controller has been developed for alleviating helicopter vibration by closed-loop implementation of higher harmonic control (HHC). This controller gives the capability to readily define many different configurations by selecting from three different control approaches (deterministic, cautious, and dual), two system models (local and global), and various methods of limiting control (e.g., external and/or internal limiting on higher harmonic pitch amplitude and rate). A representative baseline configuration has been defined for each of the three control approaches and tuned for best effectiveness at a high speed level-flight condition. After proper tuning, each baseline controller has proven very effective in reducing helicopter vibration. The following are the conclusions from this analytical evaluation study.

1) Reductions in vibration on the order of 75 to 95 percent are achieved at all significant fuselage locations for all steady flight and short duration maneuver conditions considered. These reductions are achieved for a range of both forward velocity and rotor thrust with amplitudes of 3, 4, and 5/rev control on the order of 1.0 degree or less.

2) For short duration maneuvers, the controllers remain stable, maintain peak vibration response well below uncontrolled levels, and reduce vibration to the same levels achieved at steady flight conditions. Retuning of the controllers is required to achieve satisfactory performance during some maneuvers. The results for the maneuvers investigated indicate the need for further evaluation during extended continuous maneuvers.

3) No distinct advantage in terms of controller performance has been identified for the deterministic and cautious control approaches at the flight conditions investigated. The dual controller, while equally effective in reducing vibration, tends to have slightly worse short term control and somewhat more oscillatory behavior due to system probing.

4) The baseline deterministic and cautious controllers are relatively insensitive to less than optimum tuning of internal parameters, which can be used to affect convergence characteristics, effectiveness in reducing vibration, and the magnitude of final control inputs. The dual controller is more sensitive to the tuning of internal parameters.

5) The global and local system models result in similar controller performance at steady flight conditions, but controllers based on the local model are generally less effective without retuning during short duration maneuvers.

6) Increases in rotor blade stresses and a degradation in rotor performance have been noted at most flight conditions investigated. The presence and characteristics of multiple low vibration HHC solutions suggest that alleviation of these adverse effects may be accomplished by limiting HHC to lower harmonics or by including appropriate parameters in the performance index to account for them.

References

1. Taylor, R. B.: Helicopter Rotor Blade Design for Minimum Vibration. NASA CR-(to be published), NASA, Ames, Contract NAS2-11025, UTRC Report R83-915783-27, December 1983.

2. Blackwell, R. H.: Blade Design for Reduced Helicopter Vibration. Journal of the American Helicopter Society, Vol. 28, No. 3, July 1983.

3. Bartlett, F. D.: Flight Vibration Optimization Via Conformal Mapping. Journal of the American Helicopter Society, Vol. 28, No. 1, January 1983.

4. Johnson, W.: Self-Tuning Regulators for Multicyclic Control of Helicopter Vibration. NASA Technical Paper 1996, March 1982.

5. Wood, E. R.; Powers, R. W.; and Hammond, C. E.: On Methods for Application of Harmonic Control. Fourth European Rotorcraft and Powered-Lift Aircraft Forum, September 1978.

6. McHugh, F. J.; and Shaw, J.: Benefits of Higher Harmonic Blade Pitch: Vibration Reduction, Blade Load Reduction, and Performance Improvement. Proceedings of the American Helicopter Society Mideast Region Symposium on Rotor Technology, August 1976.

7. Sissingh, G. J.; and Donham, R. E.: Hingeless Rotor Theory and Experiment on Vibration Reduction by Periodic Variation of Conventional Controls. NASA SP352, February 1974.

8. Shaw, J.; and Albion, N.: Active Control of the Helicopter Rotor for Vibration Reduction. Paper No. 80-68, 36th Annual Forum of the American Helicopter Society, Washington, D.C., 1980.

9. Taylor, R. B.; Farrar, F. A.; and Miao, W.: An Active Control System for Helicopter Vibration Control by Higher Harmonic Pitch, presented at the AIAA/ASME/ASCE/AHS 21st Structures, Structural Dynamics Conference, AIAA Paper 80-0672, May 1980.

10. Taylor, R. B.; Zwicke, P. E.; Gold, P.; Miao, W.: Analytical Design and Evaluation of an Active Control System for Helicopter Vibration Reduction and Gust Response Alleviation. NASA CR-152377, July 1980.

11. Hammond, C. E.: Wind Tunnel Results Showing Rotor Vibratory Loads Reduction Using Higher Harmonic Blade Pitch. Journal of the American Helicopter Society, Vol. 28, No. 1, January 1983.

12. Molusis, J. A.; Hammond, C. E.; Cline, J. H.: A Unified Approach to the Optimal Design of Adaptive and Gain Scheduled Controllers to Achieve Minimum Helicopter Rotor Vibration. Presented at the 37th Annual Forum of the American Helicopter Society, New Orleans, LA, May 1981.

13. Shaw, J.: Higher Harmonic Blade Pitch Control; A System for Helicopter Vibration Reduction. Massachusetts Institute of Technology, PhD Thesis, May 1980.

14. Molusis, J. A.; Mookerjee, P.; and Bar-Shalom, Y.: Evaluation of the Effect of Vibration Nonlinearity on Convergence Behavior of Adaptive Higher Harmonic Controllers. NASA CR-166424, January 1983.

15. Molusis, J. A.: The Importance of Nonlinearity on the Higher Harmonic Control of Helicopter Vibration. Presented at the 39th Annual Forum of the American Helicopter Society, St. Louis, Missouri, May 1983.

16. Chopra, I.; and McCloud, J. L., III: A Numerical Simulation Study of Open-Loop, Closed-Loop and Adaptive Multicyclic Control Systems. Journal of the American Helicopter Society, Vol. 28, No. 1, January 1983.

17. Wood, E. R.; Powers, R. W.; Cline, J. H.; and Hammond, C. E.: On Developing and Flight Testing a Higher Harmonic Control System. Presented at the 39th Annual Forum of the American Helicopter Society, May 1983.

18. Davis, M. W.: Refinement and Evaluation of Helicopter Real-Time Self-Adaptive Active Vibration Controller Algorithms. NASA CR-(to be published), NASA, Ames, Contract NAS2-11260, UTRC Report R83-956149-16, November 1983.

19. Biggers, J. C.; and McCloud, J. L., III: A Note on Multicyclic Control by Swashplate Oscillation. NASA TM-78475, April 1978.

20. Bielawa, R. L.: Aeroelastic Analysis for Helicopter Rotors with Blade Appended Pendulum Vibration Absorbers - Program User's Manual. NASA CR-165896, June 1982.

21. Bryson, A. E., Jr.; and Ho, Y. C.: Applied Optimal Control. Blaisdell Publishing Co., Waltham, MA, 1969.

22. Goodwin, G. D.; and Payne, R. L.: Dynamic System Identification, Experiment Design and Data Analysis. Academic Press, New York, 1977.

23. Wittenmark, B.: Stochastic Adaptive Control Methods, A Survey. International Journal of Control, Vol. 21, No. 5, 1975.

24. Niebanck, C.: A Model Rotor Test Data for Verification of Blade Response and Rotor Performance Calculations. USAAMRDL-TR-74-29, May 1974.